Optics Communications 344 (2015) 43–50

Contents lists available at ScienceDirect

Optics Communications

journal homepage: www.elsevier.com/locate/optcom

Detailed numerical investigation of the interaction of longitudinal acoustic waves with fiber Bragg gratings in suspended-core fibers

Ricardo E. Silva [a,b,c,*], Alexander Hartung [a], Manfred Rothhardt [a], Alexandre A.P. Pohl [c], Hartmut Bartelt [a,b]

[a] Leibniz Institute of Photonic Technology (IPHT), Albert-Einstein-Str. 9, 07745 Jena, Germany
[b] Friedrich Schiller University Jena (FSU), Fürstengraben 1, 07743 Jena, Germany
[c] Federal University of Technology-Paraná (UTFPR), Av. Sete de Setembro 3165, 80230901 Curitiba, Brazil

ARTICLE INFO

Article history:
Received 17 November 2014
Received in revised form
11 January 2015
Accepted 12 January 2015
Available online 13 January 2015

Keywords:
Acousto-optical devices
Microstructured fibers
Fiber optics components
Fiber Bragg gratings

ABSTRACT

The interaction between longitudinal acoustic waves and fiber Bragg gratings in suspended-core optical fibers is numerically investigated. The fiber core size and the air hole size are varied, and the mechanical and grating properties are simulated by means of the finite element method and the transfer matrix method, respectively. Changes of the effective index, confinement factor, silica area, strain and wavelength shift induced by the acoustic wave are evaluated, and the resultant side lobe reflectivity is estimated. A side lobe reflectivity increase of 66% compared to standard fibers is estimated, which allows reducing the modulation index or the grating length in as much as 75%. Besides, the larger reduction of the required acoustic power for achieving the acousto-optic modulation points out to more efficient modulator devices in suspended-core fibers.

1. Introduction

The interaction of longitudinal acoustic waves and fiber Bragg gratings (FBGs) allows the dynamic change of the reflectivity and the wavelength of reflection bands in both sides of the Bragg resonance, which is useful for the control of tunable reflectors, modulators and also the inscription of gratings [1–8]. If the side lobe is used as a mirror in a laser cavity, the acoustic modulation can be applied to tune the power and the operating wavelength of fiber lasers [7].

Fig. 1 illustrates how the acousto-optic interaction with longitudinal waves takes place. First, if an optical mode with effective index n_{eff} propagates in a non-perturbed fiber containing a grating of period Λ, this mode will interact with the grating structure, resulting in a reflected band at the Bragg wavelength $\lambda_B = 2n_{eff}\Lambda$ (Fig. 1(a)). However, if a longitudinal acoustic wave is excited along the fiber axis z, it produces a periodic strain, which compresses and stretches the grating. In this way, the strain modulates the mode effective index $n_{eff}(z)$ and the grating period $\Lambda(z)$, causing lobes to appear on both sides of the Bragg wavelength (Fig. 1(b)). The normalized side lobe reflectivity η is given as [1,2,9],

$$\eta = \tan h^2\left[\frac{\pi \Delta n_{ac}\Gamma}{\lambda_B} L J_m\left(\frac{\lambda_a}{\Lambda}S\right)\right]. \quad (1)$$

Here, S is the peak strain, J_m is the Bessel function of the first kind of order m, Δn_{ac} is the grating index modulation amplitude, L is the grating length, λ_a is the acoustic period and Γ is the fraction of the optical power into the propagating mode that overlaps with the grating. For the step index single mode optical fiber (SMF) the peak strain S can be approximated as [2],

$$S = \sqrt{\frac{2P_{ac}}{EA_s v}}, \quad (2)$$

in which P_{ac} is the acoustic power, E is the Young's modulus, A_s is the silica fiber cross section and v is the acoustic velocity. For a specific value of $P_{ac,}$ it should be noted that in Eqs. (1) and (2) the reflectivity η can be increased by increasing the index modulation Δn_{ac} or the grating length L, as well, by reducing the cladding diameter.

In a continuously excited standard single mode fiber, the acoustic power is evenly distributed over the whole fiber cross section. This leads to a reduced overlap between the acoustic power and the Bragg grating causing the reduction of the reflectivity η. Cladding-etched fibers with strong gratings or tapered fibers with long gratings enhance the acousto-optic interaction and, hence, the reflectivity η [1,2,7]. In the first case, the

* Corresponding author at: Leibniz Institute of Photonic Technology (IPHT), Albert-Einstein-Str. 9, 07745 Jena, Germany
E-mail address: ricardoezq@yahoo.com.br (R.E. Silva).

http://dx.doi.org/10.1016/j.optcom.2015.01.037
0030-4018/

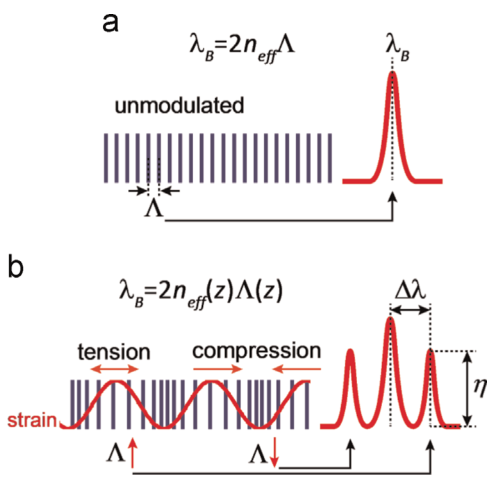

Fig. 1. Behavior of the fiber Bragg grating (a) without and (b) with longitudinal acousto-optical modulation.

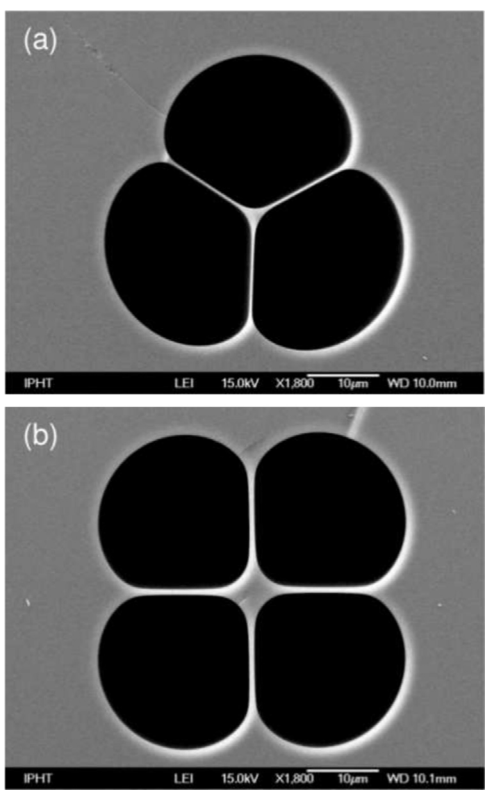

Fig. 2. Cross section of the supendend core fibers with (a) three and (b) four air holes used as model for the simulations.

inscription of strong gratings requires higher power densities, germanium dopants or hydrogen loading [9]. In addition, a higher grating modulation index Δn_{ac} can also limit the side lobe operation wavelength, since the FBG bandwidth should be kept smaller than the distance between the main Bragg resonance and the side lobe in order to avoid overlap. In the second case, the inscription of long gratings is limited by the spatial and temporal coherence of interferometry techniques (e.g. Talbot interferometer) or implies the use the long phase masks or additional equipment to shift the fiber or the laser beam [9]. Moreover, the experimental realization of tapers is laborious, mainly due to the relatively long fiber transitions required to efficiently increase the acousto-optic interaction. In addition, the reduction of the fiber diameter makes the optical properties more susceptible to surface contamination and affects its mechanical stability [10].

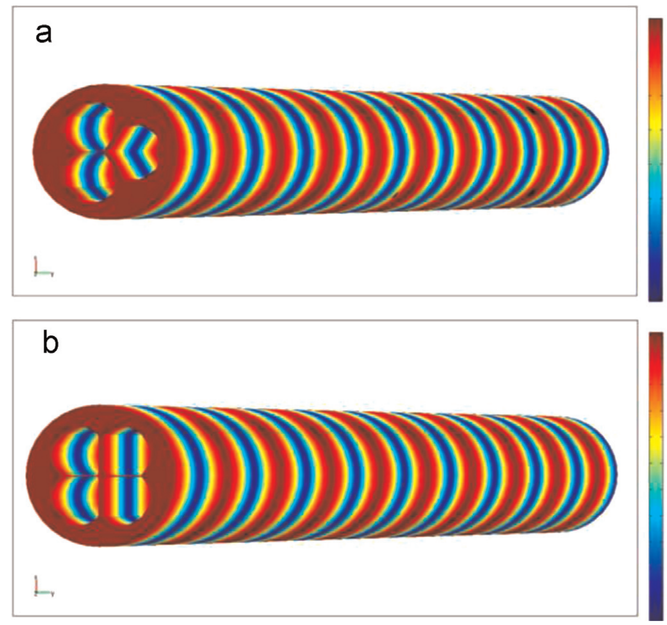

Fig. 3. Exemplary 3D simulation of the displacement distribution for (a) SCF3 and (b) SCF4 excited in the core by a longitudinal acoustic wave.

On the other hand, suspended-core fibers (SCFs) have a small core in size suspended by thin walls and surrounded by a single ring of large air holes [11–15]. This allows reducing of the amount of silica in the cladding, which leads to increase the acousto-optic interaction between the longitudinal acoustic wave and the Bragg grating in the core. Given this condition, we numerically investigate in this paper the influence of the core and the air hole sizes of different suspended-core fibers upon the acousto-optic interaction. By simulating the modal and mechanical fiber properties along with the grating properties, we verified that the reflectivity η can be significantly increased compared to standard fibers, while the mechanical stability and shielding against environmental influences are further maintained. It relaxes the requirements for inscribing strong or long gratings and avoids the cladding reduction by etching or taper techniques. Compared to standard fibers, the increased reflectivity in suspended-core fibers also allows a reduction of size and of power consumed by acousto-optic devices.

2. Methodology

The simulations are conducted by means of a 3D finite element method (FEM), which is provided by the software package Comsol Multiphysics®. For the simulation of the acoustic wave, Young's modulus $E = 72.5$ GPa, Poisson's ratio $\sigma = 0.17$ and the density $\rho = 2200\ \mathrm{kg/m^3}$ for silica are considered [16]. The methodology used to evaluate the strain induced in the core by the longitudinal acoustic wave is described elsewhere [4,8]. The FEM is also used to simulate the modal properties, such as the effective index n_{eff} of the fundamental mode and the confinement factor Γ. The FBG spectrum is simulated by means of the transfer matrix method [5] considering an initial grating of index modulation $\Delta n_{ac} = 10^{-4}$, a reflectivity of $R \sim 99\%$ and a Bragg wavelength centered at $\lambda_B = 1550$ nm. The FBG and the fiber length is 25 mm in both cases.

Fig. 2(a) and (b) show a cross section of two real SCFs fabricated at the Institute of Photonic Technology which served as the initial model for the subsequent calculations. Fig. 2(a) shows the SCF3 composed of three air holes of $\delta = 27\ \mu$m in diameter separated by